High resolution near-field acoustic holography

HIGH RESOLUTION NEAR-FIELD ACOUSTIC HOLOGRAPHY

Rick Scholte[1,2], N.B. (Bert) Roozen[2,1]

[1]Philips Center for Industrial Technology
P.O. Box 218
5600 MD Eindhoven, The Netherlands
e-mail address of lead author: Rick.Scholte@Philips.com

[2]Eindhoven University of Technology, Mechanical Engineering
P.O. Box 513
5600 MD Eindhoven, The Netherlands

Abstract

High resolution Near-field Acoustic Holography (NAH) is not a widely discussed topic in open literature. For instance articles on automotive or naval applications do not discuss resolutions beyond one centimetre. Electronic appliances on the other hand demand a high spatial resolution, since the components of printed circuit boards become smaller and smaller. These applications require a spatial resolution in the order of millimetres. As an example, components such as Surface Mounted Devices (SMDs) carry high frequent switching voltages, which may have a noise generating effect. Even sound power levels as low as 30 dB(A) can be annoying to the customer, requiring a diagnostic tool such as NAH to localise the sound source(s) of relatively low acoustic levels at a high spatial resolution. To obtain high-resolution acoustic images, the acoustic signal processing and measurement set-up have to be tuned carefully. The paper focuses upon the determination of optimal measurement and reconstruction parameters to enable highly accurate source reconstructions, which in this case are limited to stationary, coherent sources only. To illustrate the high-resolution capabilities of Planar Near-field Acoustic Holography (PNAH) a test case is used. The test case is a plate containing three baffled sources, each two millimetre in diameter, half a millimetre apart. The measurements show that the sources are identified with sub-millimetre resolution.

INTRODUCTION

One of the main interests of Planar Near-field Acoustic Holography (PNAH) on small objects is the maximum achievable resolution of the acoustic field information at the source plane. This resolution depends on a number of parameters that can be set either by the measurement or the post-processing properties. The different parameters affecting the resolution of the acoustic images will be discussed in this chapter. Also a post-processing algorithm to determine the optimal k-space filter parameters will be introduced. The work of Williams [1] is used as a basis for PNAH acoustic signal processing.

THEORETICAL SPATIAL RESOLUTION

Spatial sampling

Sampling in the spatial domain is determined by the acoustic sensor positions. The distances Δx and Δy between the measurement positions on the measurement plane make up the spatial discretisation and can be seen as a spatial AD-conversion. The Nyquist criterion [2] for analogue to digital signal processing is equally valid in the spatial domain. Consider a noise-free acoustic measurement in the near-field. The minimum distance between two acoustic sensors or spatial samples determines the maximum observable wavenumber, k_{max}. The minimum observable wavelength is 2 samples long, or

$$\lambda_{\min} = 2\Delta x \qquad \text{[m]}. \tag{1}$$

This makes the highest observable wavenumber:

$$k_{\max} = \frac{2\pi}{\lambda_{\min}} \qquad \text{[rad/m]}. \tag{2}$$

The resolution of an acoustic image can be defined as the minimum distance between two acoustic sources that can be observed. This minimum change in acoustic quantity can at best be observed by two neighbouring sensor positions of which one is, for example, sensing a high sound pressure and the other a low sound pressure. In the noise-free case the resolution of the acoustic image will be

$$R_{\max} = \frac{\lambda_{\min}}{2} = \frac{\pi}{k_{\max}} = \Delta x \qquad \text{[m]}. \tag{3}$$

Thus, the maximum resolution of the acoustic image is at first determined by the sensor distance, which is the absolute upper boundary and should be chosen with care. So, if the sensor distance is too large compared to the wavenumbers one is interested in the process will fail and the resolution will not be adequate. A second bounding

property for the maximum resolution of an acoustic image is the signal-to-noise ratio, which will be discussed in the next paragraph.

Influence of measurement noise on resolution

In case there are no evanescent waves available from the measurements and the grid spacing is smaller than $2\Delta x$, the resolution R is determined by the free field acoustic wavelength λ:

$$R_{\min} = \frac{\lambda}{2} \qquad [\mathrm{m}]. \tag{4}$$

This can be defined as the minimum resolution for an acoustic image, which, in fact, is the resolution that can be obtained by beam-forming or acoustic holography. In practise the resolution that can be obtained by PNAH will be in-between R_{min} and R_{max}. To increase the spatial resolution beyond R_{min}, it is clear that a measurement in the near-field of the object is necessary to acquire information about the evanescent waves.

The error level of an actually measured hologram contains some intrinsic error, also referred to as noise, which includes background sound, diffraction from the microphone, electric noise, calibration errors, etc. Interesting information about the noise is the difference between signal and noise, also known as signal-to-noise ratio (SNR), or dynamic range D, which is defined as

$$D = 20^{10}\log\left(\frac{M}{E}\right), \tag{5}$$

where M is the maximum measured field amplitude and E is the noise amplitude. This is an important quantity because the dynamic range D influences the maximum observable wavenumber as a function of the source-hologram distance (z_h-z_s). From [3] we know that we can write

$$R = \frac{\pi}{\sqrt{k^2 + \left(\frac{D\ln 10}{20(z_h - z_s)}\right)^2}} \tag{6}$$

for the resolution of the acoustic image that is possible with dynamic range D. For D=0dB there are no evanescent waves available and R is equal to the resolution obtained by beam-forming, R_{min} in (4). So, the better the dynamic range of your measurement, the higher the resolution of your acoustic image when measuring in the near-field.

The potential of NAH is a direct result of the dynamic range with which the evanescent waves are measured in the near-field. Compared to beam-forming or acoustic holography, NAH will result in a much higher resolution given a high dynamic range. Consider for example the acoustic radiation at a single angular frequency of $\omega_s=2\pi 1000$ rad/s at different distances z_h-z_s. The resolution of the acoustic image depends on the dynamic range D as shown in Figure 1, where the

upper graph gives the resolution for beam-forming where no resolution improvement is obtained for higher dynamic range. From (4) and $\omega_s=2\pi1000$ rad/s it follows that $R_{min}=0.17$ m.

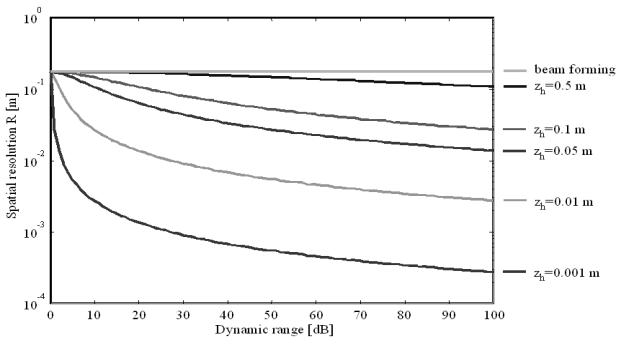

Figure 1: Influence of Dynamic range and hologram distance on resolution for $\omega_s=2\pi1000$ rad/s.

These graphs tell us that distance from acoustic sensors to the source should be as small as possible (but not too small, as will be seen in the next section) and the dynamic range of the measurement should be as large as possible in order to maximize resolution.

Spatial aliasing

An important issue when acquiring a holographic measurement is the distance from the tip of the sensor to the source plane, or as stated above: z_h-z_s. From (6) we know that the resolution strongly depends on this distance and decreasing it will boost resolution. There are two main reasons why decreasing the hologram distance z_h-z_s has its limits.

The first reason is the influence of the sensor on the acoustic behaviour of the source. Diffraction and a change in acoustic impedance can be of great importance on short distances. The second reason is the spatial sampling spacing, or Δx and Δy. The spatial sampling and hologram distance are interlinked because of aliasing effects. Aliasing is a well-known issue in digital signal processing and is a result of the under-sampling of data. Take for example the sine wave with a high wavenumber as illustrated in Figure 2. This sine wave is sampled by Δx, which results in the sampling points marked by the black dots.

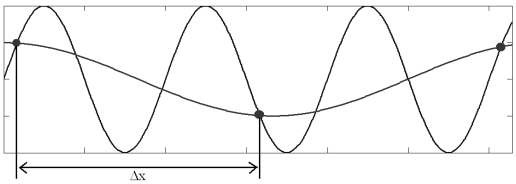

Figure 2: Under-sampling of a sine wave.

When only considering the sampled data, which is the only data available after acoustic array measurements, the sine wave that fits these points has a much larger wavelength (also illustrated in Figure 2). Thus, spatial aliasing causes an inability to reconstruct the exact sound field.

In time domain digital signal processing, typically, a low-pass filter applied before sampling is used to ensure that frequencies higher than half the sampling frequency are not present. However, it is not possible to apply an analogue filter for spatial acoustic data because the high wavenumbers are present in the near-field of the source and cannot be suppressed without interrupting the acoustic properties of the field between source and hologram plane. A spatial low-pass filter can be made effective by a proper choice of the hologram distance, since the highest observable wavenumber is dependant on this distance. Because it is assumed that sources only exist in the half space z<0, there is no source that could produce higher wavenumbers at the hologram plane, for a given distance to the source. This can be seen as a natural anti-aliasing filter.

Coupling of spatial sampling, hologram distance and dynamic range

In accordance with the Nyquist criterion we have seen that $0.5k_{sample}$ is the maximum observable wavenumber in a noise free environment. A noise free environment implicates that $D \to \infty$ and the resolution R from (6), which considers the effect of measurement noise on the resolution only, becomes approximately zero. This effect is limited by the "other" resolution from (3) due to spatial sampling. When the inequality,

$$\sqrt{k^2 + \left(\frac{D\ln 10}{20(z_h - z_s)}\right)^2} \succ 0.5k_{sample}, \tag{7}$$

is true, aliasing occurs. In other words, there exists a distance $z_h - z_s$ below which, at a certain dynamic range, aliasing occurs at a chosen spatial sampling frequency, because from this distance on evanescent waves higher than the Nyquist wavenumber are observable. Inequality (7) couples spatial sampling, hologram distance and dynamic range, which makes it possible to wisely set your measurement parameters. Figure 3 illustrates inequality (7). It also shows that the frequency of the signal plays an unimportant role.

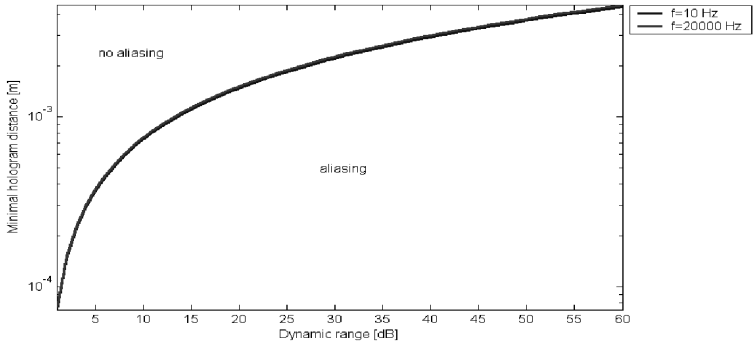

Figure 3: Spatial aliasing due to dynamic range and hologram distance.

SPATIAL RESOLUTION MEASUREMENT

Measurement

In order to verify the above stated properties and limitations of spatial PNAH resolution, a measurement is performed. The set-up is pictured in Figure 4a and b. The object comprises three holes in a baffled plate. The three holes, each with a 2 mm diameter, are positioned in line, 0.5 mm apart. A cylindrical cavity is connected to all three holes and the cylindrical cavity is connected to a closed speaker box, which results in in-phase acoustic waves coming out of the holes.

a) holes in aluminium plate

b) plate in baffle

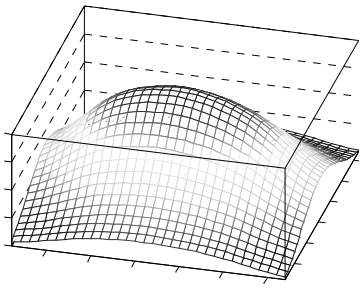

c) Measured hologram at 3 mm and f=2365Hz

Figure 4: Measurement information

The hologram distance z_h-z_s is 3 mm and the spatial sampling distance in both x- and y-direction is 0.3 mm, which is based on (7), a dynamic range of approximately 45dB and the required resolution of at least 0.5 mm. The hologram as illustrated in Figure 4c should give us enough information to reconstruct all three sources.

Post-processing and L-curve Regularization in PNAH

The acoustic hologram is partly processed as illustrated by the block diagram in Figure 5.

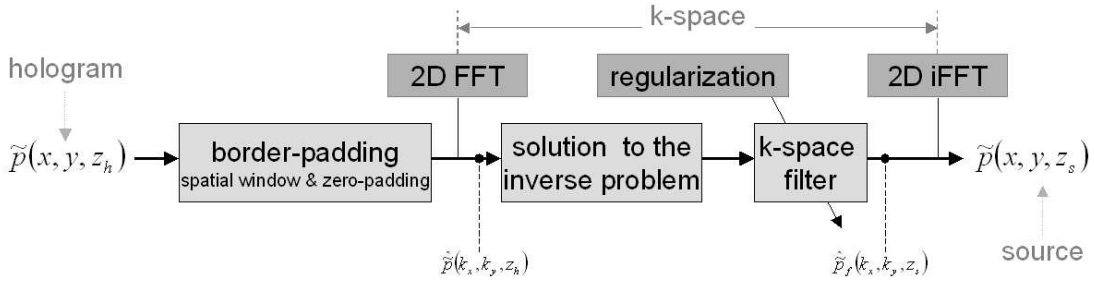

Figure 5: Block diagram of PNAH post-processing

The basics of this technique are described in [1], an expansion with zero- and border-padding is described in [4], and a thorough description of the full post-processing strategy and its performance can be found in [5].

Extra attention is necessary for the low-pass k-space filter and especially its regularization. Since an increasingly higher k_{co} results in a "blow up" of the result, the k-space filter cut-off variation is a good measure for application of an L-curve.

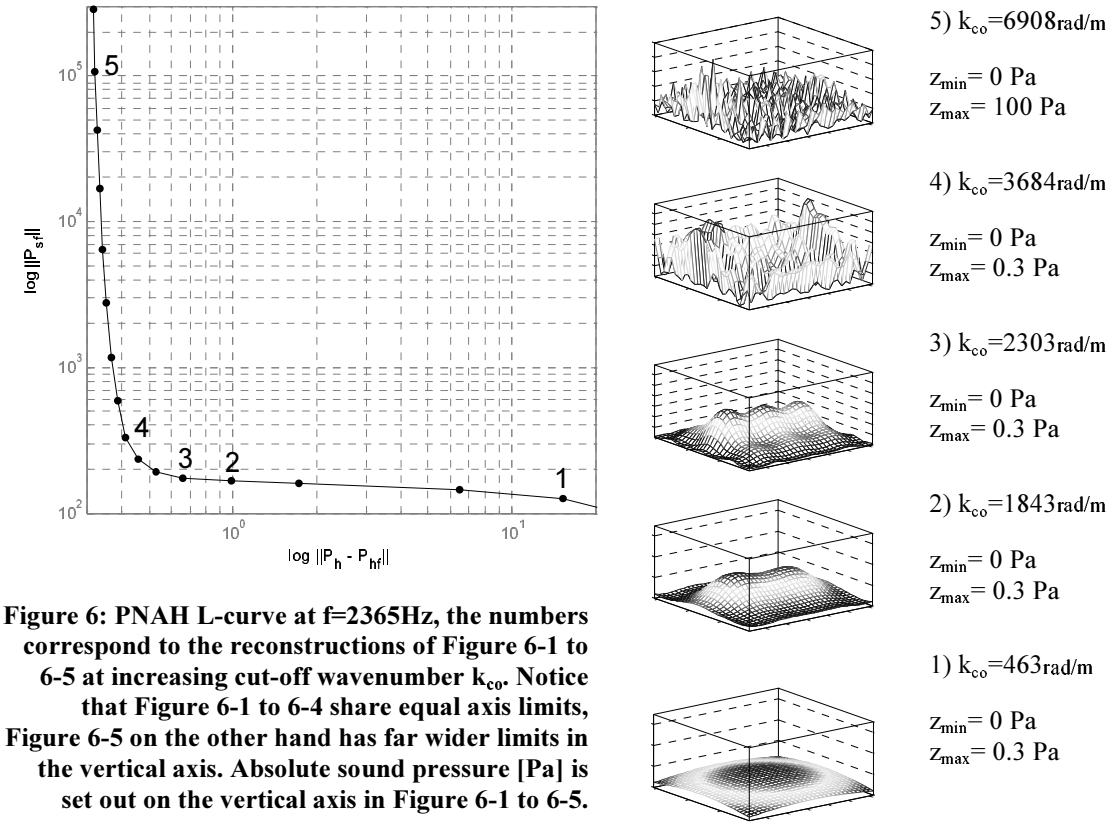

Figure 6: PNAH L-curve at f=2365Hz, the numbers correspond to the reconstructions of Figure 6-1 to 6-5 at increasing cut-off wavenumber k_{co}. Notice that Figure 6-1 to 6-4 share equal axis limits, Figure 6-5 on the other hand has far wider limits in the vertical axis. Absolute sound pressure [Pa] is set out on the vertical axis in Figure 6-1 to 6-5.

In [6] a clear description of the L-curve and its usefulness in inverse problems, like in PNAH, is given. In short, the application of the L-curve shows the switch between underestimation of the inverse solution by too much low-pass filtering (the right, horizontal part of the "L") and the "blow up" of the solution by the lack of low-pass filtering (the left, vertical part of the "L"). Optimal regularization can be obtained by selecting a cut-off value that corresponds to the corner of the L-curve. The "blow up" effect by PNAH can be properly described by the norm of the k-space counterpart of the spatial sound pressure result: $\left\|\hat{\tilde{p}}_f(k_x,k_y,z_s)\right\|$. The effect of a too tight k-space filter can also be determined properly in k-space by taking the norm of the hologram counterpart in k-space minus the low-pass filtered version, or $\left\|\hat{\tilde{p}}(k_x,k_y,z_h)-\hat{\tilde{p}}_f(k_x,k_y,z_h)\right\|$. Now, we plot $\left\|\hat{\tilde{p}}_f(k_x,k_y,z_s)\right\|$ versus $\left\|\hat{\tilde{p}}(k_x,k_y,z\ )-\hat{\tilde{p}}_f(k_x,k_y,z\ )\right\|$ in a log-log graph, resulting in the L-curve of Figure 6.

The effects of the low-pass filter are clearly visible in Figure 6-1 to 6-5. Position one shows the reconstruction of the source with a very low cut-off, resulting in only one recognizable source. The cut-off of position two is still too low, but now two sources are recognized. When cut-offs become too high in case of position 4 and 5, the reconstruction becomes very inaccurate since noise has blown up. When we observe the L-curve and choose the proper position in the corner of the "L", the properly regularised result is obtained where the three individual sources can be recognized.

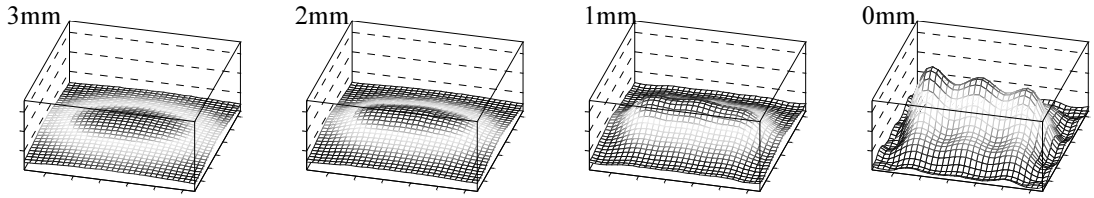

Figure 7: From left to right: absolute sound pressure [Pa] from hologram to source, k_{c0}=2303rad/m corresponding with Figure 6-3.

The spatial change from the hologram plane at 3 mm in steps of 1 mm to the source plane at 0 mm can be observed from left to right in Figure 7. Since the axis share equal limits, the change from a distance of just 3 mm with only one recognizable source to a distance of 0 mm with three recognizable sources is clearly visible.

SUMMARY

This work shows that a spatial resolution between 0.5 and 1 mm is possible by means of proper measurements and improved PNAH post-processing techniques. The coupling of spatial sampling theory, dynamic range and knowledge of aliasing conditions prove to be very important in the set-up of a PNAH measurement. From a post-processing point of view the application of an L-curve for PNAH is very effective and helpful in the determination of the optimal cut-off for the k-space filter.

REFERENCES

[1] E.G. Williams, *Fourier Acoustics. Sound and Nearfield Acoustical Holography* (Academic Press, 1999)

[2] H. Nyquist, "Certain Topics in Telegraph Transmission Theory", AIEE **Trans., 47,** 617-644 (1928)

[3] J.D. Maynard, E.G. Williams, Y. Lee, "Nearfield acoustic holography: I. Theory of generalised holography and the development of NAH", J.Acoust. Soc. **Am., 78 (4)** (1985)

[4] R. Scholte, N.B. Roozen, "Improved data representation in NAH applications by means of zero-padding", 10th Intern. congress on sound and vibration, Stockholm, Sweden (2003)

[5] R. Scholte, "Improved Source Localization Techniques in Planar Nearfield Acoustic Holography", Master Thesis University of Twente, Philips CFT, Eindhoven, The Netherlands (2004)

[6] P.C. Hansen, "The L-curve and its use in the numerical treatment of inverse problems" (1999)